Journal of Structural and Construction Engineering, 11(1), 2024, pp. 05-25

Journal of Structural and Construction Engineering

www.jsce.ir

Durability of Alkali-activated Slag/Pumice Mortars in Mineral Acid Environments: Effects of Pumice Powder and Activator Type

Mohsen Jafari Nadoushan [1], Rasoul Banar[2], Pooria Dashti[2], Amirmohammad Ramezanianpour[3,*]

1- Assistant Professor, Department of Civil Engineering, Faculty of Civil and Earth Resources Engineering, Central Tehran Branch, Islamic Azad University, Tehran, Iran
2- PhD Candidate, Department of Civil & Environmental Engineering, Amirkabir University of Technology, Tehran, Iran
3- Associate Professor, Faculty of civil engineering, College of Engineering, University of Tehran, Tehran, Iran

ABSTRACT

Nowadays, one of the most desirable alternatives to cement-based composites is the alkali-activated blends which can be towards achieving more durable materials. In alkali-activated slag/pumice (AASP) mortars, ground granulated blast-furnace slag (GGBFS) could be replaced partially with Volcanic pumice powder (VPP) as a natural pozzolan; however, its performance in alkali-activated slag/pumice (AASP) mortars against mineral acid environments are currently missing in the literature. In this paper, the durability of AASP mortars containing 0 or 10% VPP activated by the combination of sodium silicate with NaOH or KOH exposed to a high concentration of sulphuric and nitric acids were investigated. In addition to flowability, capillary water absorption, and mercury intrusion porosimetry tests, deterioration due to the mineral acid attack was examined using visual condition assessment, mass loss, compressive strength change, and X-ray diffraction analysis (XRD). A comparison was also performed with ordinary Portland cement (OPC) mortar specimens as a reference mixture. It was found that the AASP mortars are more durable than a corresponding OPC mortar in terms of mass and compressive strength changes in sulphuric and nitric acid solutions. Generally, employing 10% VPP exhibited no significant effect on the durability of AASP mortars against mineral acid attack. In addition, utilizing NaOH alkali activator could be a better choice in exposure to sulphuric acid, but in nitric acid solution, KOH-activated samples revealed better durability in terms of mass and compressive strength change.

ARTICLE INFO

Receive Date: 09 May 2023
Revise Date: 08 July 2023
Accept Date: 11 July 2023

Keywords:
Alkali-activated blends
Sulphuric acid
Nitric acid
Volcanic pumice powder
Slag
XRD

doi: https://doi.org/10.22065/jsce.2023.396256.3111

*Corresponding author: Amirmohammad Ramezanianpour.
Email address: ramezanian@ut.ac.ir

1. Introduction

The mineral or inorganic acids are derived from an inorganic compound that gets separated in water to produce hydrogen ions (H+). Mineral acids such as sulphuric and nitric acids are corrosive environments [1]. So, resistance to acid attack is one of the essential durability properties in building materials exposed to acidic environments. One of the most prevalent deteriorations of concrete is its deterioration in aggressive acidic media. The vulnerability of ordinary Portland cement (OPC) concrete to acid attack is related to a high amount of calcium hydroxide (CaOH) and its solubility in acid solution, and hydrogen ions also expedite the leaching of CaOH. In relatively high concentrations of acids, the C-S-H structure is attacked, and silica gel is formed [2]. Several researchers suggested alkali-activated binders have the potential to be an alternative to cementitious binders. There are two different alkali-activated materials (AAMs), including low calcium and high calcium binders. Complete replacement of fly ash, metakaolin, rice husk ash, and natural pozzolans with ground granulated blast-furnace slag (GGBFS) in alkali-activated slag (AAS) binders (high-calcium binders) provides the production of alkali-activated low-calcium binders called geopolymers. In order to take advantage of both types of AAMs, future researchers tend to use hybrid low-calcium and high-calcium binders [3].

Several advantages of AAMs such as high early strength, low rate of energy consumption, low CO2 emission, promising durability performance in aggressive situations, and low creep have made them suitable alternatives to Ordinary Portland Cement (OPC) binders [4]. One of the most suitable properties of AAMs is their relatively high resistance in acidic media compared to OPC binders discussed by several researchers [5-7].

The mechanism of deterioration of AAMs subjected to acidic media is believed to be related to depolymerization of aluminosilicate polymers, silicic acid release, the substitution of cations (i.e., K+ and Na+) by H+ or H3O+ and leaching of aluminium, and condensation of siliceous polymers and zeolites. Different modes of deterioration may occur in AAMs immersed in acidic media depending on the level of materials performance; high-performance materials deteriorate due to the development of fissures in the amorphous polymer matrix because of fragmentation of alumino-silicate gel in acid as a result of Si-O-Si and Si-O-Al bondings breakage; however, crystallization of zeolites in the non-crystalline matrix may cause low-performance materials deterioration [8].

Studies on the corrosion mechanism of geopolymer pastes in high concentrations of sulphuric and nitric acids demonstrated a two-step process. At first, irrespective of the type of acid, the alkali cations are replaced by H+ and H3O+ from the acid solution, and tetrahedral aluminum ejects from the structure due to the electrophilic attack on Si-O-Al bondings. In the second step, the re-occupation of vacancies by Si occurs in nitric acid solution, and forms an imperfect framework. However, in sulphuric acid, the reaction of calcium ions with sulphate anions results in the formation and deposition of crystalline gypsum in the framework [9, 10].

Geopolymer mortar specimens are reported to remain structurally intact after 24-week immersion in high concentration nitric acid solution. The higher content of alkali in activators is responsible for their better performance. Mass loss and compressive strength change in geopolymer materials are related to the diffusion of calcium and sodium ions from the framework. Investigations on the microstructure demonstrated that the porosity of geopolymer materials decreased due to the accumulation of deterioration products during the acid attack [11, 12]. Bernal et al. [13] Claimed that diluted mineral acids had a negligible effect on compressive strength change in Portland cement and silicate activated slag mortars, while organic acids had more destructive effects. [14] and [15] showed that the addition of fly ash in AAS mixes led to better resistance against acid attack due to the decrease of calcium and lime content in the matrix. There are some limited studies on the performance of alkaline activation of hybrid GGBFS and natural pozzolan binders [16-19].

Literature review suggests that the durability performance of alkali-activated mixes containing GGBFS and natural pozzolan mortars exposed to mineral acids has yet to be investigated. In the authors' preliminary study [18], the optimal level of replacing GGBFS by volcanic pumice powder (VPP) was determined as 10% (by mass) in terms of flowability and compressive strength. This study aims to assess the durability of four mix designs of alkali-activated slag/pumice (AASP) mortars in high concentration sulphuric and nitric acids considering the effects of two factors: 1) 10% replacement of VPP natural pozzolan by GGBFS, 2) the type of alkali activator (NaOH and KOH). Deterioration was examined using evaluation of specimens' visual condition, mass loss, compressive strength change, and X-ray diffraction (XRD) of specimens. In addition, flowability, capillary water absorption, and mercury intrusion porosimetry (MIP) tests have been conducted. A comparison was also made with OPC mortar specimens as a reference mixture.

2. Experimental Program

2.1. Materials

Ground granulated blast-furnace slag (GGBFS) and a natural pozzolan, namely volcanic pumice powder (VPP) from Taftan Mountains were used as base materials. Table 1 shows the chemical characteristics and the physical properties of raw materials. Figure 1 shows the XRD patterns of GGBFS and VPP. Two types of alkali activators including sodium hydroxide

(NaOH) and potassium hydroxide (KOH) pellets were dissolved in deionized water to obtain a 6 molar alkaline solution to be used as activators. Water glass or sodium silicate (SS) was provided in the form of a solution with the modulus (i.e., the mass ratio of SiO2 to Na2O) of 2.33. Silica sand fine aggregates were used in this study. Figure 2 shows the particle size distribution of the silica sand and the specification for standard sand according to ASTM C778 [20][20][20][20][20].

Ordinary Portland cement was used to prepare a reference mixture. The cement's chemical characteristics and physical properties are shown in Table 2 and Table 3, respectively. The ordinary Portland cement met the specifications presented in ASTM C150 [21][21][21][21][21]. In order to enhance the flowability of the OPC mortar, a polycarboxylate-based superplasticizer was added to the reference mixture to achieve almost the same flowability as other AASP mixtures. Sulphuric and nitric acids were used as acidic media to evaluate the durability of AASP and OPC mortars. Table 4 shows the characteristics of sulphuric and nitric acids.

Table 1. Chemical characteristics and physical properties of raw materials.

Chemical Components (%)	GGBFS	VPP
Calcium oxide (CaO)	36.75	7.4
Silicon oxide (SiO_2)	37.21	64.9
Mangnesium oxide (MgO)	8.52	1.98
Aluminum oxide (Al_2O_3)	11.56	12.1
Ferric oxide (SO_3)	1.01	5.2
Sodium oxide (Na_2O)	0.61	2.49
Potassium oxide (K_2O)	0.7	1.88
Titanium dioxide (TiO_2)	1.23	0.79
Manganese oxide (MnO)	0.99	0.123
Phosphor pentaoxide (P_2O_5)	0.03	0.2
Loss on ignition (LOI)	0.02	2.5
Physical properties		
Blaine Fineness (cm^2/gr)	3383	5047
Specific Gravity (gr/cm^3)	2.79	2.54

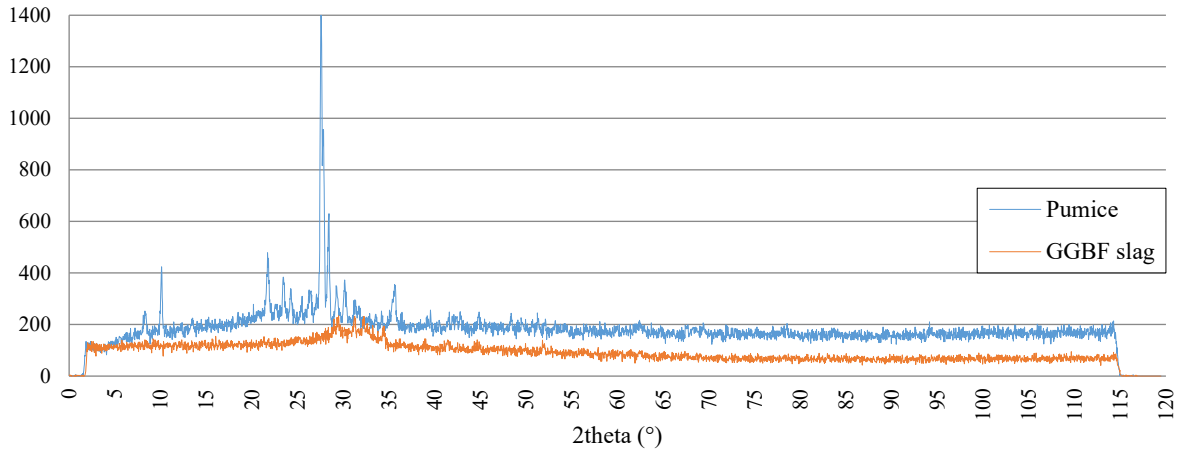

Figure 1. XRD patterns of GGBFS and VPP.

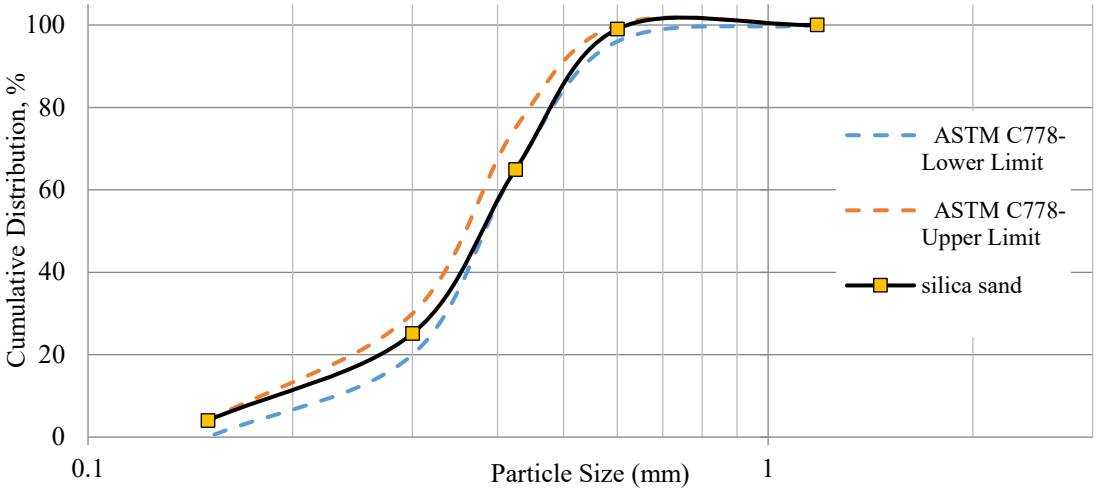

Figure 2. Particle size distribution of silica sand.

Table 2. Chemical characteristics of OPC.

Chemical Compositions	Percentage	Compound Components	Weight (%)
CaO	63.78	C_3S	45.6
SiO_2	21.55	C_2S	27.39
Al_2O_3	5.89	C_3A	9.31
Fe_2O_3	3.72	C_4AF	11.32
SO_3	1.89		
MgO	1.35		
Na_2O	0.53		
K_2O	0.3		
LOI	0.94		

Table 3. Physical properties of OPC.

Property	Quantity
Specific Gravity (gr/cm^3)	3.02
Blaine Fineness (cm^2/gr)	3035
Material Passing Sieve 45µm (%)	86.28
Initial Setting Time (min)	145
Final Setting Time (min)	185

Table 4. Characteristics of used mineral acids.

Characteristic	Acid Type	
	Sulphuric Acid (95-98%)	Nitric Acid (65%)
Chemical Formula	H_2SO_4	HNO_3
Type	Extra Pure	Extra Pure
Specific Gravity (gr/cm^3)	1.84	1.40
Molecular Weight (gr/mol)	98.08	63.01

2.2 Mixture Proportion

Two factors related to the properties of the AASP mortars, i.e., the type of alkaline solution and GGBFS replacement ratio with VPP natural pozzolan were investigated. The level of each factor and their values were chosen based on the authors' previous researches [18, 22]. AASP and OPC mortar mixture proportions are shown in Table 5 and Table 6, respectively. Considering that the total amount of solid materials except sand in AASP mortars was equal to 592.60 kg/m3, the cement content in OPC mortar was considered equal to the same amount. The water to cement ratio in the OPC mortar was considered equal to 0.487 concerning the ratio of water to solid materials in the AASP mortars.

Table 5. AASP mortar mixtures proportions.

No.	Mix.	AS	Molarity	Raw Material (kg/m^3)	GGBFS Replacement with VPP (%)	Modulus of SS	Activator to raw material	Aggregate to raw material	Water to solid
1	Na6-Pu0	NaOH	6	463.8	0	2.33	0.9	2.75	0.487
2	Na6-Pu10	NaOH	6	463.8	10	2.33	0.9	2.75	0.487
3	K6-Pu0	KOH	6	463.8	0	2.33	0.9	2.75	0.418
4	K6-Pu10	KOH	6	463.8	10	2.33	0.9	2.75	0.418

AS: alkali solution, SS: sodium silicate

Table 6. OPC mortar mixture proportions.

No.	Mix	Cement (kg/m^3)	Water to Cement	Aggregate to Cement	Superplasticizer dosage (% of Cement weight)
5	OPC	592.6	0.487	2.75	0.3

2.3 Mixing Procedure and Specimen Preparation

In order to produce the AASP mortar mixtures, sodium or potassium hydroxide pellets were added to deionized water to achieve 6 molar solutions. Raw materials (GGBFS and VPP) were mixed in dry condition. NaOH or KOH solution and water glass were added to the raw materials, and the mixture was blended for 30 seconds. After 15 seconds of interruption, aggregates were added and mixed for 60 seconds. Then, after 15 seconds of relaxation, mixing was continued for another 60 seconds. The prepared AASP mortar was transferred to steel 50×50×50 mm dimension moulds. Then, the AASP mortars were compacted by using a vibration table for 10-30 seconds. Specimens were kept protected after casting to avoid water evaporation for 24 hours. Next, the specimens were removed from the mould and cured in dry plastic bags for 25 days. In the last step, specimens were saturated in freshwater for 3 days and then transferred to the acidic media. The OPC mortar was mixed according to ASTM C305[23][23][23][23][23]. Then, it was cast in steel 50×50×50 mm dimension moulds. The specimens were then compacted using vibration table for about 10-30 seconds. Specimens were kept protected after casting to avoid water evaporation for 24 hours. OPC mortar specimens were transferred to the acidic media after 28 days of water curing. The AASP and OPC mortar specimens were exposed to sulphuric and nitric acid solutions with pH=1. The Acidic

media was prepared by adding fresh water to pure acid to obtain the desired pH. The acid concentration was monitored via titration and by a portable digital pH meter whenever it was necessary (at the first days because of considerable change, pH was being monitored daily, and after 2 weeks, it was being monitored at weekly intervals), and concentrated acid was added to the solution to maintain the pH level within the desired range of concentration (pH=1). All of the experiments were done at room temperature of 23 ±1 celcius.

2.4 Test Procedure

The flowability of fresh AASP and OPC mortars was determined according to ASTM C1437[24][24][24][24][24]. The capillary water absorption test was performed following the BS EN 480-5 standard [25][25][25][25][25]. For this purpose, prismatic samples of AASP and OPC mortar with dimensions of 160 × 40 × 40 mm were made and cured up to the age of testing in a chamber with a relative humidity of 65±5 % and a temperature of 20 ± 2 Celsius. This test was performed on AASP and OPC mortar samples at 3, 7, 28, and 91 days. Moreover, the pore size distribution and total porosity of mortars were comparatively measured by mercury intrusion porosimetry (MIP) following ASTM D 4404-10 using PASCAL 440 and PASCAL 140 porosimeters (Fig. 3). Based on the pressure range of the used equipment, pore diameters between 5 nm to 50 µm could be evaluated. For this purpose, after 91 days of moist curing, the samples were cut into 1 cm cubes, dried in air, and then tested.

Since there is no standard test method for assessing the resistance of mortars to acid attack, in this study, all mortar specimens were immersed in sulphuric and nitric acid solutions of pH=1 after 28 days of casting. For assessing the performance of AASP and OPC mortars in mineral acid solutions, visual inspection, mass change, compressive strength change, and XRD tests were conducted. In order to evaluate the mass change in acid, the mass of the specimens was measured at weekly intervals in saturated surface dry conditions; two samples of each mix design were measured for mass change evaluation. Samples were washed by water and soft brush, and then their surfaces were dried to determine their weight with a ±0.01 gr precision. After the measurement, specimens were immersed in acid again. Spacers were used to ensure complete immersion of samples in the acid environment.

The compressive strength of 50×50×50 mm AASP and OPC mortar specimens was determined at 0, 7, 28, and 91 days of exposure to acid according to ASTM C109 [26][26][26][26][26]. Two samples of each mix design were tested for compressive strength, and in the case of considerable difference, the third sample was tested to meet the desired precision.

X-ray diffraction (XRD) analysis was performed on control specimens and those exposed to acid after 91 days using an Equinox300 X-ray diffractometer operating at 40 kV and 30 mA.

Figure 3. Porosimeter PASCAL 440 and Porosimeter PASCAL 140.

3. Results and Discussion

3.1. Flowability

Figure 4 presents the flowability of fresh mortars. AASP mortars containing KOH showed higher flowability than mortars containing NaOH. The higher flowability of mortars activated by KOH is contrary to expectations because, at the same molarity, KOH solution has a lower water/binder ratio than NaOH solution. Due to the greater extent of dissolution of alumina-silicate minerals in KOH solution, the flowability of AASP mortars containing KOH is higher than NaOH ones. The more solid alkali content in KOH mortars has led the hardening of the mixtures to be attained through the geopolymerization process, which usually occurs at a slower rate as compared with the C-S-H formation process [27, 28]. Replacement of GGBFS with VPP reduced flowability of AASP mortars containing NaOH or KOH due to a relatively higher amount of specific surface area of VPP than GGBFS (5074 cm^2/gr vs. 3383 cm^2/gr). A similar issue has been reported in the research of Najimi et al. [3], stating that the higher specific surface area causes more water demand to reach constant flowability. Overall, the flowability of AASP mortars was higher than OPC mortar. These results were in accordance with other previous studies [29, 30].

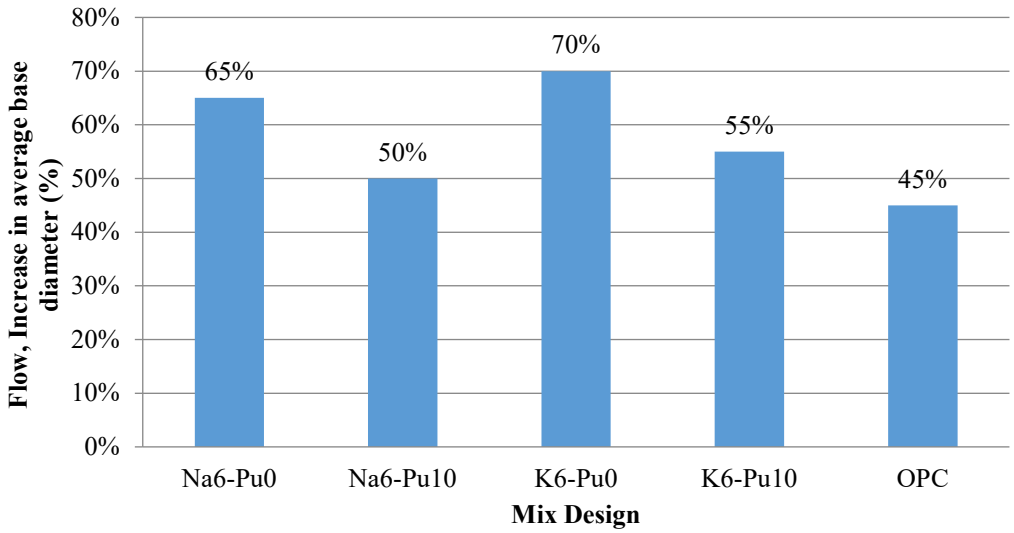

Figure 4. The flow of the fresh AASP and OPC mortars.

3.2. Capillary water absorption

Figure 5 shows the capillary water absorption of the mortars at various ages. As can be seen, the capillary water absorption of AASP mortar samples was much lower than that of the OPC mortar sample at all ages. This is due to the denser matrix, fewer capillary pores, and more curvature of cavities in AASP mortars relative to OPC mortar [31-34]. One of the main reasons for this issue is the consumption of water during the hydration of Portland cement, while in the geopolymerization reaction, some water is released, which leads to the densification of geopolymer mixtures compared to cement-based mixtures [35, 36]. It was also observed that at early ages, the capillary water absorption of AASP mortars containing NaOH was less than samples containing KOH, but at later ages, the results for AASP mortar samples were closer. Although the results of capillary water absorption of AASP mortar samples had a minor difference, it can be said that samples containing 10% VPP and 90% GGBFS had relatively less capillary water absorption than similar samples containing 100% GGBFS, especially at early ages. This can be related to the difference between the formed gels and finer particle size of the used VPP natural pozzolan compared to GGBFS. In other words, the used VPP natural pozzolan had a much finer particle size, causing it to fill the pores and lead to lower water absorption. Similar observations were reported by some past researches [3, 37, 38]. Due to the slight difference in the results of the water sorptivity test for AASP mortars, especially at later ages, the MIP test was performed for a more accurate comparison.

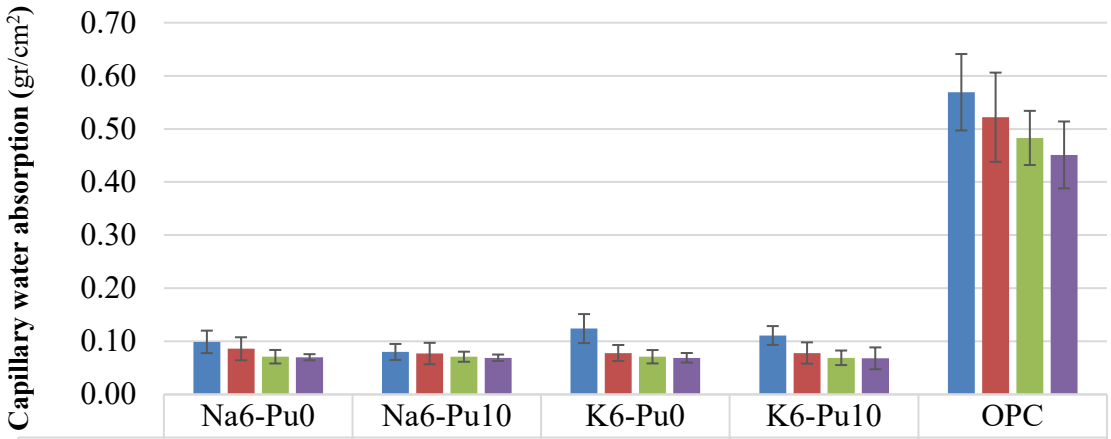

	Na6-Pu0	Na6-Pu10	K6-Pu0	K6-Pu10	OPC
3 Days	0.099	0.080	0.124	0.111	0.569
7 Days	0.086	0.077	0.078	0.078	0.522
28 Days	0.071	0.071	0.071	0.069	0.483
91 Days	0.070	0.069	0.069	0.068	0.451

Figure 5. Capillary water absorption of AASP and OPC mortar specimens.

3.3. Mercury intrusion porosimetry (MIP)

Figure 6 depicts the cumulative pore volume of AASP and OPC mortar specimens at 91 days. All specimens illustrated a continuous pore distribution within the pore size of 5 nm to 50 µm. As can be seen, all AASP mortars showed a denser structure and smaller pore size than OPC mortar. The 10 % replacement of VPP in AASP mixtures caused more porosity compared to similar mixes without VPP. This difference is more evident between Na6-Pu0 and Na6-Pu10 samples. Although the replacement of VPP with GGBFS was expected to result in a denser structure due to the finer particles, the MIP test results showed the opposite [39].

Similar to [40], a change in the slope of the cumulative distribution curve of the samples' pores occurred at about 100 nm. Therefore, 100 nm was considered as the threshold between small and large pores in the matrix, pertaining to nano-pores and micro-pores, respectively. The permeability and diffusion properties of materials were closely related to the threshold pore diameter, as it completes the pores' connectivity in materials dramatically [41, 42]. Figure 7 shows the total pore volume (5 nm-50 µm), including sizes smaller and larger than 100 nm for AASP and OPC mortars. The micro-pores volume (100 nm-50 µm) in the AASP mortars without VPP was less than those containing 10% VPP. MIP measurements proved that incorporating VPP led to increment of capillary pores more than GGBFS. This indicates that most of the chemical reactivity of VPP appeared at early ages rather than older ages (91 days). In addition, the formation of N-A-S-H type gel from the activation of VPP resulted in relatively higher porosity and less compactness relative to the microstructure of C-A-S-H gel for GGBFS [38, 43]. It can also be concluded that the pores larger than 100 nm (micro-pores) in AASP mortars activated with NaOH were less than AASP mortars containing KOH. This is due to the fact that sodium cations have a smaller size than potassium cations, thus leading to a denser microstructure of NaOH mixtures [44]. On the other hand, the results of MIP test shows that the volume of nano-pores in all samples is greater than that micro-pores, which has a greater effect on reducing the density of samples, but comparing the test results of Capillary water absorption by MIP test shows that despite the greater effect of nano-pores in the density of samples, capillary water absorption of samples is correlated with micro-pores. Among the studied mixtures, Na6-Pu0 and OPC mortars had the lowest and highest total pore volumes, respectively.

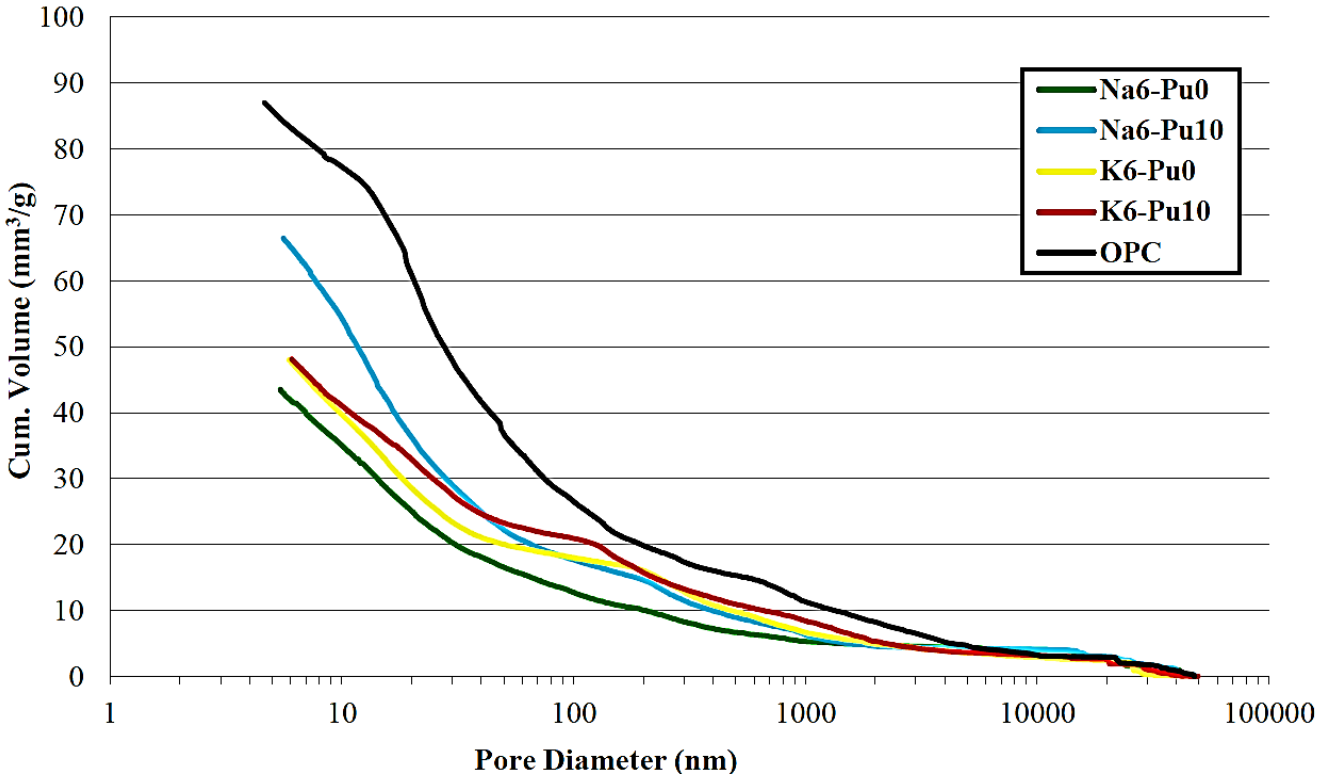

Figure 6. Results of MIP test for cumulative pore volume of mix designs from 5 nm to 50 µm.

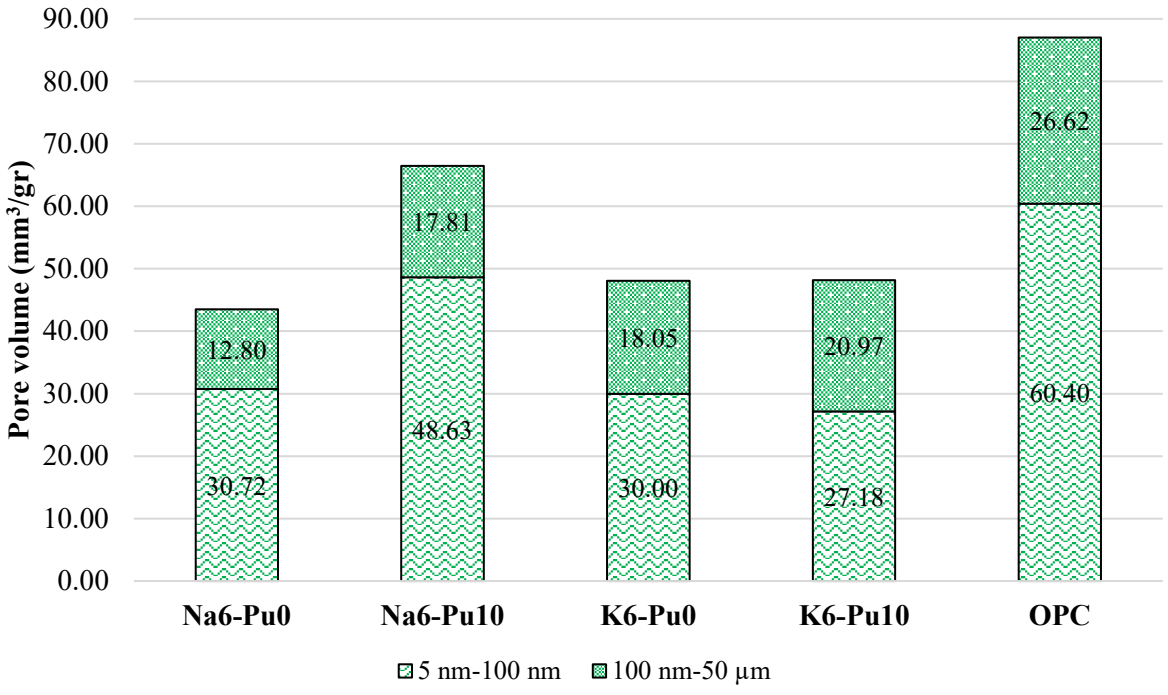

Figure 7. The classification of total pore volume (smaller and larger than 100 nm) for mix designs.

3.4. Durability against mineral acids

3.4.1. Visual Inspection

Figure 8 shows the visual condition of specimens after 56 days of immersion in acid solutions. As shown in Fig. 8, AASP mortar specimens in sulphuric acid remained structurally intact, and the formation of a hard layer reduced the permeation of acid to inner parts. It can be concluded from Fig. 8 (b) that the immersion of OPC mortar in nitric acid led to the dissolution of $Ca(OH)_2$ and calcium sulphoaluminates (AFt and AFm), and the decalcification of C-S-H with a high C/S ratio that leaves a very porous corroded layer, while the low lime content in AASP mortars resulted in a dense protective layer of silica gel [45].

After 1 month of immersion in acid, expansion was observed in AASP mortar specimens and facilitated acid diffusion into specimens, and exacerbated their degradation, as seen in Fig. 9 (a). A white thick, soft layer of gypsum was observed in OPC mortar specimens, and they deteriorated rapidly in sulphuric acid. Figure 9 (b) shows the accumulation of gypsum on the surfaces of OPC specimens. The AASP mortar specimens exposed to sulphuric acid showed expansion cracks due to the extensive formation of gypsum in the regions close to the surfaces [14, 46].

The difference in the appearance of the outer surfaces and inner parts of the AASP mortar specimen indicates a diffusion prevention mechanism in sulphuric acid, as seen in Fig. 10. Actually, the dark color of the inner parts of the AASP specimen indicates that the material has not been subjected to oxidative processes, and provides a direct indication of the very limited degree of acid ingress into the material that is consistent with the study presented by Bernal et al. [13]. No evidence of expansion, cracking, or shrinkage was observed in AASP and OPC mortar specimens immersed in nitric acid (Fig. 8 b). AASP and OPC mortar specimens in nitric acid showed relatively high porosity on the surface. Crystallization was also observed near the surface of the AASP mortar specimens exposed to nitric acid.

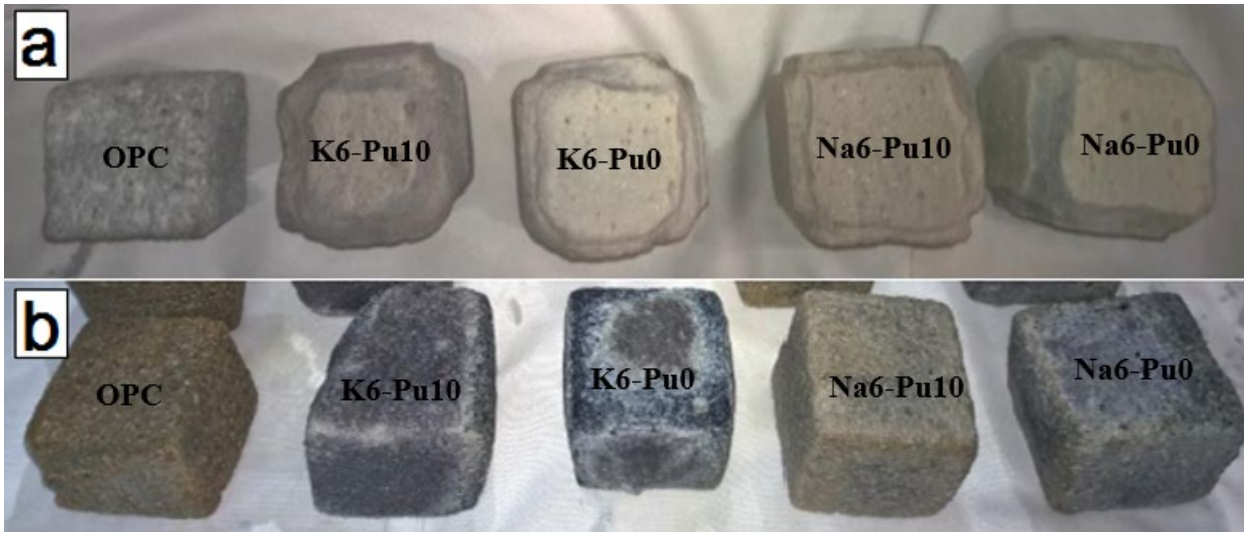

Figure 8. AASP and OPC mortar specimens after 56 days of exposure to acid media, (a) sulphuric acid solution, (b) nitric acid solution

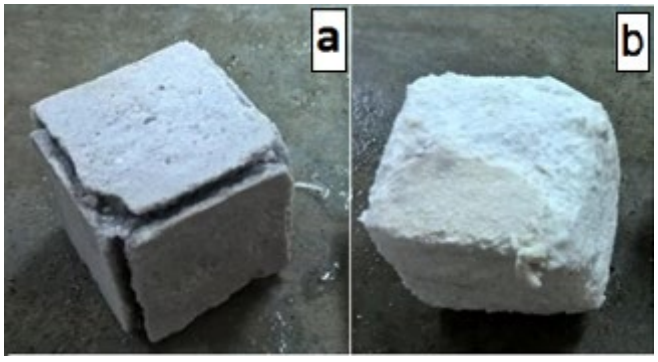

Figure 9. Deterioration of mortars in sulphuric acid after 1 month, (a) Na6-Pu0, (b) OPC mortar.

Figure 10. An example of Outer surfaces and inner parts of an AASP mortar specimen immersed in sulphuric acid after 91 days.

3.4.2 Mass Change

Figure 11 and Figure 12 demonstrate the mass change of the AASP and OPC mortar specimens in sulphuric and nitric acid solutions up to 91 days, respectively. In the sulphuric acid solution, the AASP mortar specimens had a low rate of mass loss in the first 49 days of immersion; however, deterioration was gradually expedited due to increasing expansion and acid penetration into cubes. The durability against mineral acids of the AASP mortar specimens was superior to the OPC mortar specimens. The low content of portlandite ($Ca(OH)_2$) and low rate of water absorption in AASP mortars are advantages that lead to slower degradation and better resistance as compared to OPC mortar when subjected to mineral acid environments [13, 14, 47]. It can be inferred that NaOH had a better performance as an activator in comparison to KOH in terms of mass loss of AASP mortars in sulphuric acid solution. Nevertheless, the performance of AASP mortars containing VPP natural pozzolan against mineral acids (considering mass change) was not consistent. In other words, replacing GGBFS with 10% VPP did not clearly enhance the acid resistance of AASP specimens. In the nitric acid solution, the rate of mass loss at the early days of immersion was more remarkable, and it decreased after about 21 days of immersion. As can be seen in Fig. 12, in nitric acid solution, the AASP specimens activated by KOH had relatively better acid resistance in comparison to NaOH.

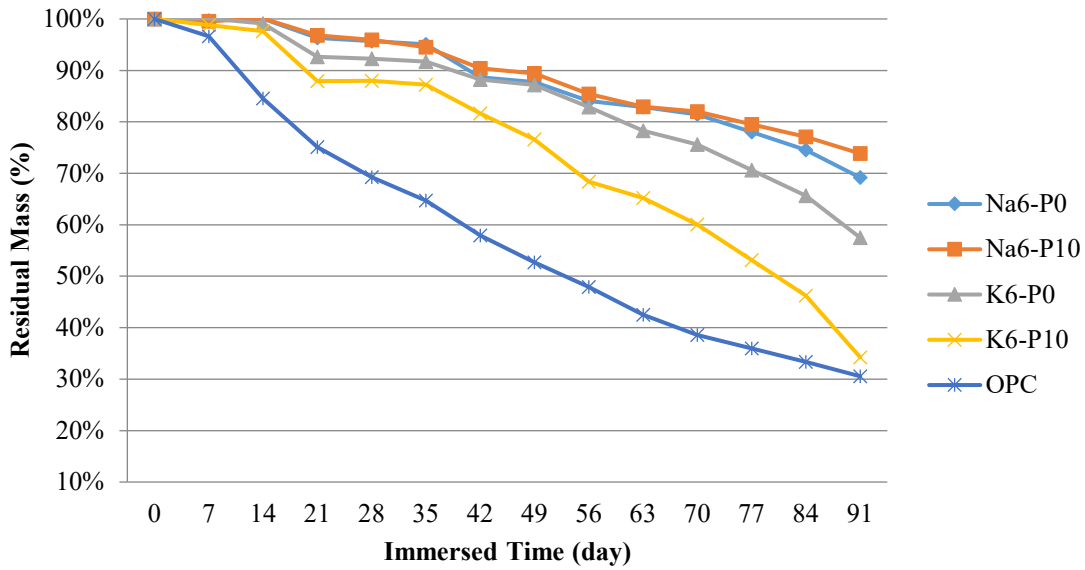

Figure 11. Mass change of the mortar specimens immersed in the sulphuric acid up to 91 days.

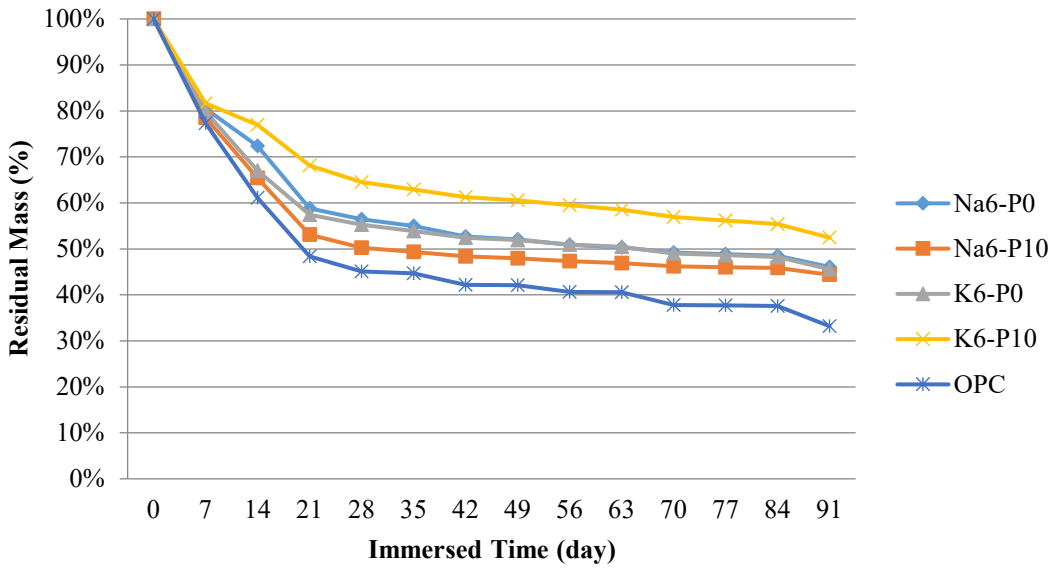

Figure 12. Mass change of the mortar specimens immersed in the nitric acid up to 91 days.

3.4.3 Compressive Strength Change

The effect of sulphuric and nitric acid attack on the residual compressive strength of AASP and OPC mortar specimens are shown in Fig. 13 and Fig. 14, respectively. Similar to the mass change results, better acid resistance of the AASP mortar specimens can be seen in comparison to the OPC mortar specimens in terms of compressive strength change. In the nitric acid media, fluctuation of the compressive strength of AASP and OPC mortar specimens can be seen in Fig. 14. It may be attributed to the progress of geopolymerization reactions and the effect of acid attack. In the AASP mortars, the presence of KOH as an activator caused better nitric acid resistance in comparison to NaOH. The replacement of GGBFS with VPP also enhanced acid resistance in nitric acid solution. This may be attributed to reduction in the calcium content in binders with the replacement of GGBFS by VPP, which makes the binder further resistant to acid attack [14, 15]. Comparing the results of mass change and compressive strength change in acidic media, it can be inferred that mass change results were relatively more reliable than compressive strength change results. Because, unlike compressive strength specimens, the used specimens for mass change were non-destructive and the same during the experiment. Comparing the residual compressive strength of OPC sample in sulphuric and nitric acids illustrated relatively better performance of OPC exposed to nitric acid. It can be attributed to the formation of different reaction products in this two mineral acids. The prominent product of OPC mortar after immersion in sulphuric acid is calcium sulphate (CaSO4) which resulted in lower compressive strength. But in nitric acid ambient, calcium silicon nitrate (Ca_4SiN_4) formed as a main product. This matter is further discussed in Section 3.4.4.

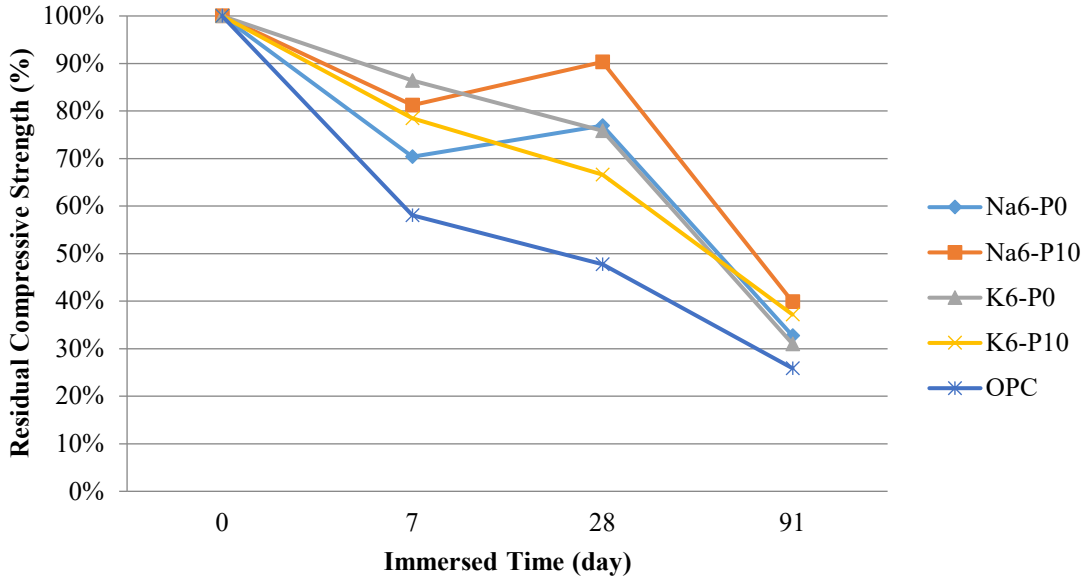

Figure 13. Compressive strength change of mortar specimens immersed in sulphuric acid up to 91 days.

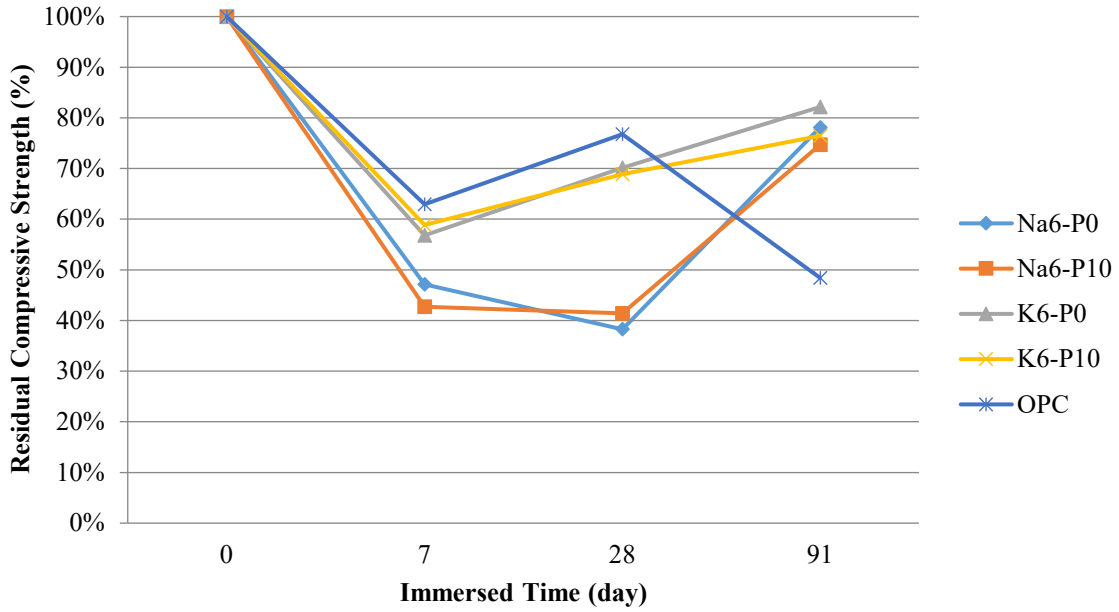

Figure 14. Compressive strength change of mortar specimens immersed in nitric acid up to 91 days.

3.4.4 X-Ray Diffraction (XRD)

Figures 15-17 show the XRD spectra for all 5 mortar samples in three categories; 1) not affected by acid, 2) immersed in sulphuric acid, and 3) immersed in nitric acid. Peaks for quartz (SiO_2) and nepheline ($(Na,K)AlSiO_4$) and albite ($NaAlSi_3O_8$) can be seen in Fig. 15 for AASP mortars. Also, quartz, calcite ($CaCO_3$), and portlandite ($Ca(OH)_2$) were observed in OPC mortars. According to the results shown in Fig. 15, all AASP mortars had the same phases and the main peaks (nepheline) for them were at around 2θ equal to 26°. Similar spectra for alkali-activated slag and cement-based mortars were reported in Türker et al.'s research [48]. The peak intensity for mixtures containing VPP was higher than mixtures without VPP. Comparing results of XRD spectra and MIP demonstrated that nepheline phase growth due to the use of VPP could increase the porosity of AASP mixtures. For mixtures exposed to sulphuric acid after 91 days, it could be seen that some nepheline and albite had transformed to sodium and potassium sulphate (Na_2SO_4 and K_2SO_4), as observed by Elyamany et al. [49]. This change in composition was associated with expansion and subsequent destruction of mortar samples. Comparing Fig. 16 and

Fig. 17 displays that sulphuric acid had a higher effect on mortars samples than nitric acid, due to more changes in the composition of the mortars. The results of Fig. 17 show that nitric acid changes the nepheline and albite in AASP mixes to sodium and potassium nitrite ($NaNO_2$ and KNO_2), which is associated with expansion and destruction of mortar samples, which is similar to the sulphuric acid environment but with less intensity. In the case of OPC mixtures in sulphuric acid, it is clear that gypsum ($CaSO_4$) was formed, dominating the calcite and portlandite peaks, which caused expansion in OPC mortar specimens. Some calcite peaks were present in the nitric acid solution, and calcium silicon nitrate (Ca_4SiN_4) appeared in XRD spectra due to the acidic attack. Similar to gypsum, calcium silicon nitrate could cause an expansion in OPC mixtures and reduce the stability of mixtures [50].

Ne: Nepheline, Al: Albite, Qu: Quartz, Ca:Calcite, Po: Portlandite

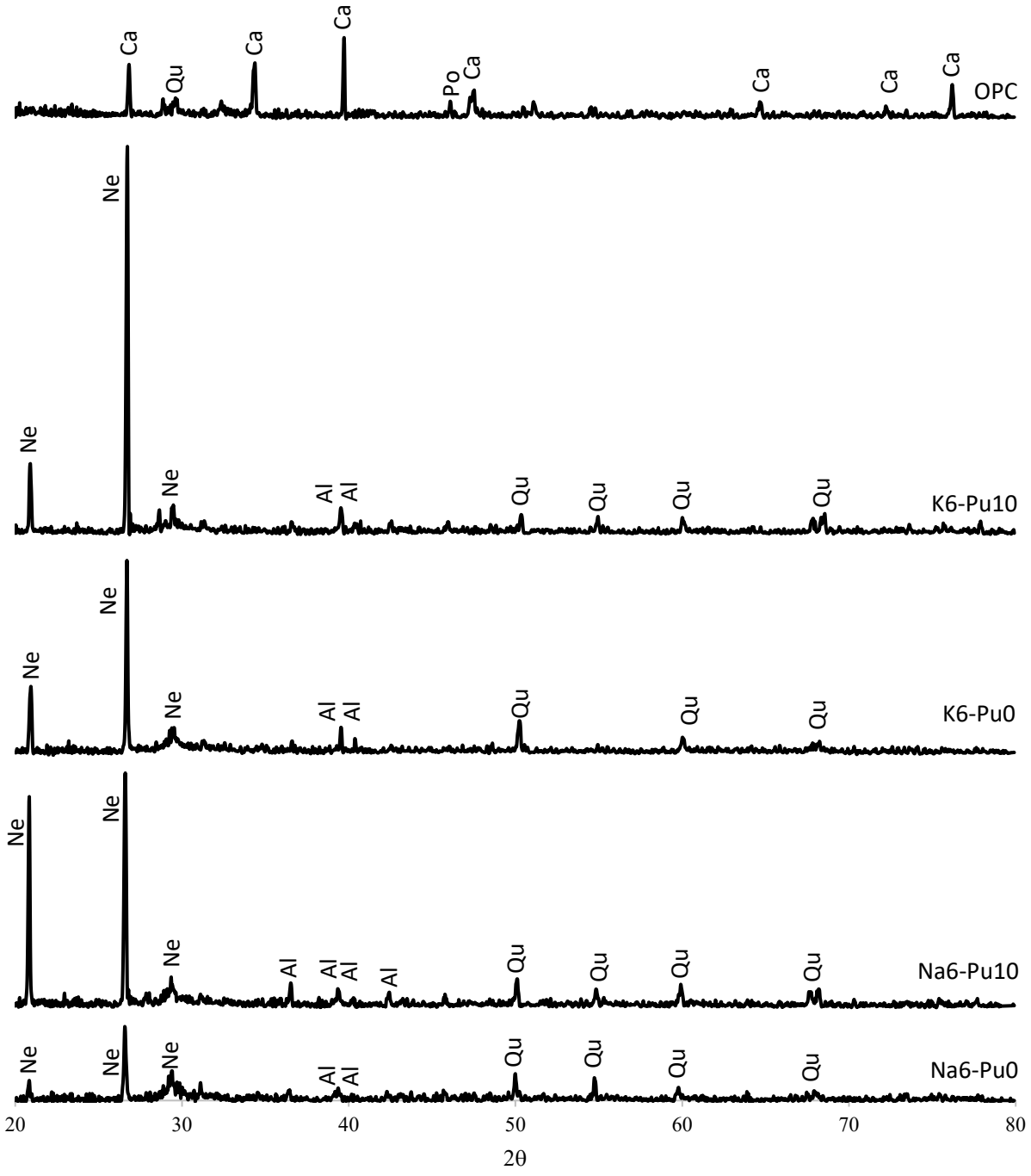

Figure 15. XRD pattern of mortar samples not affected by acid at 91 days.

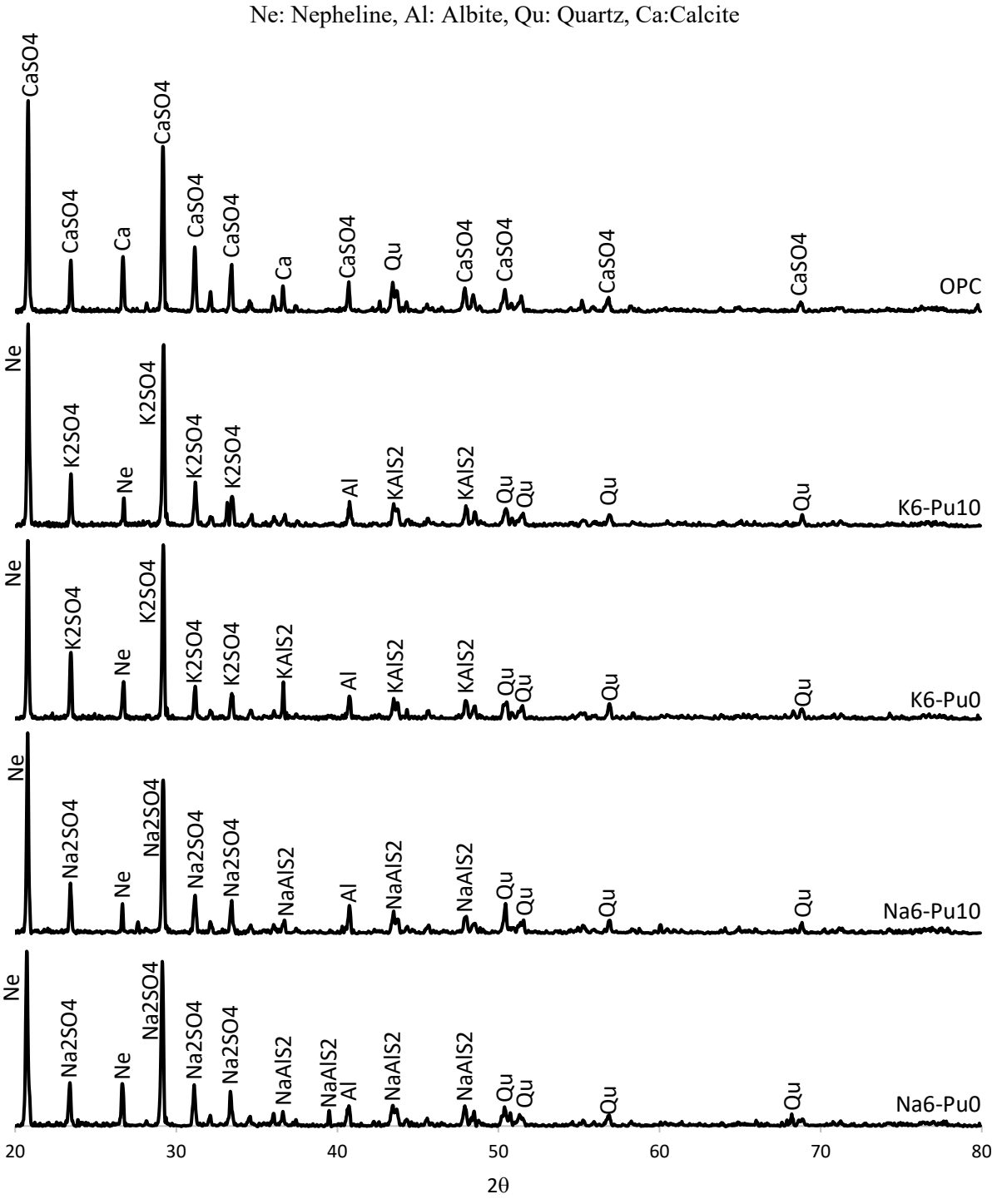

Figure 16. XRD pattern of mortar samples immersed in sulphuric acid for 91 days.

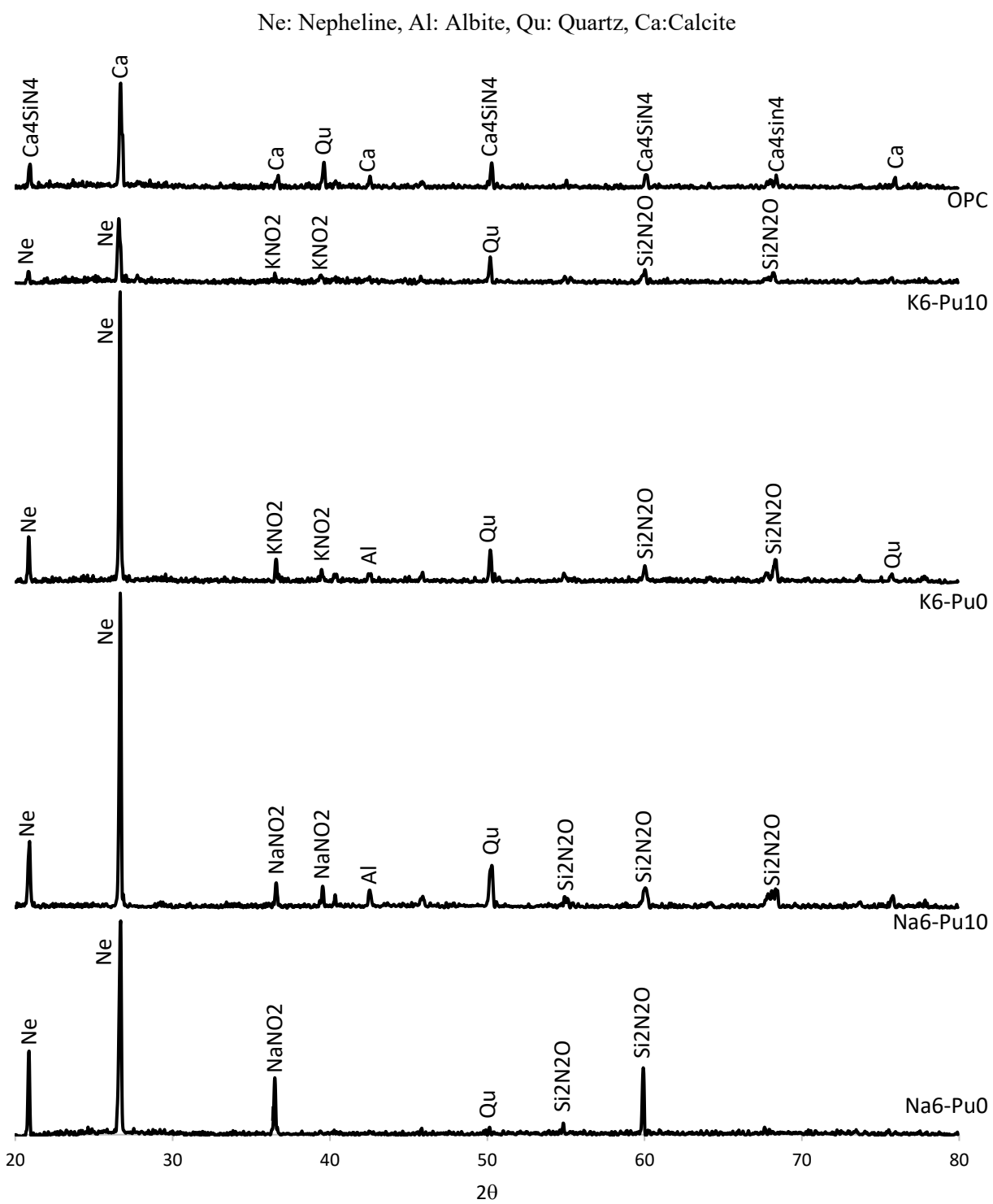

Figure 17. XRD pattern of mortar samples immersed in nitric acid for 91 days

3.5. Discussion

This section provides an evaluation of the effect of using VPP and the type of alkaline solution on mass and compressive strength changes of AASP mortars during the acidic attack at 91 days by statistical analysis. For statistical analysis, laboratory test results were compared by paired samples t-test (α=0.05). The results of this analysis are summarized in Table 7 and Table 8 for variables of VPP and type of alkaline solution, respectively. According to Table 7, the use of 10%

VPP in mortars containing NaOH activator had no significant effect on mass loss of samples exposed to both sulphuric and nitric acids. In contrast, the effect of utilizing 10% VPP was more significant in KOH-activated mixes, resulting in a considerable mass loss in sulphuric acid in samples containing VPP and KOH activator (K6-Pu10). According to the results of section 3.3 (Fig. 7), due to the higher amount of micro-pores in K6-Pu10, it was expected that this mixture would have the lowest durability against the acidic environment, especially sulphuric acid. Also, there was a discernible difference between samples containing VPP and samples without VPP in terms of residual strength after exposure to an acidic environment. In general, utilizing 10% VPP as a GGBFS substitution in AASP mortars had no significant influence on their durability in acidic environments. The significant difference observed in mass loss between samples K6-P0 and K6-P10 might be related to the destruction of edges and corners of specimens owing to stress concentration. Usually, the corrosion created on the surfaces of the samples gathers together at the edges and corners and causes the stress concentration, which results in more breakage and damage in the corners and edges compared to the sample surfaces. Moodi et al. [51] noted this reason for the sharp mass loss in samples exposed to destructive environments. As mentioned previously, the mass change results were relatively more reliable than compressive strength change results in AASP mortars exposed to mineral acids. The residual strength results did not show any difference between variables of the mix designs. Table 8 shows that the alkaline activator had a significant effect on the mass loss of AASP mortars; however, its effect was different for the sulphuric and nitric acid environments.

Table 7. VPP replacement effect based on the statistical analysis

Condition	**Sulphuric acid**				**Nitric acid**			
Variable: Pumice (%)	0	10	0	10	0	10	0	10
Mixture	Na6-Pu0	Na6-Pu10	K6-Pu0	K6-Pu10	Na6-Pu0	Na6-Pu10	K6-Pu0	K6-Pu10
Residual mass (%)	69	74	57	34	46	44	46	52
"t" calculated	0.12		30.06		0.03		3.24	
Residual Strength (%)	33	40	31	37	78	75	82	76
"t" calculated	2.23		0.96		2.17		0.86	
"t" critical	4.30							

Table 8. Type of alkali solution effect based on the statistical analysis.

Condition	**Sulphuric acid**				**Nitric acid**			
Variable: Alkaline Solution	NaOH	KOH	NaOH	KOH	NaOH	KOH	NaOH	KOH
Mixture	Na6-Pu0	K6-Pu0	Na6-Pu10	K6-Pu10	Na6-Pu0	K6-Pu0	Na6-Pu10	K6-Pu10
Residual mass (%)	69	57	74	34	46	46	44	52
"t" calculated	2.25		12.66		0.4		5.12	
Residual Strength (%)	33	31	40	37	78	82	75	76
"t" calculated	0.92		1.21		0.58		0.88	
"t" critical	4.30							

Table 9. The solubility of chemical compounds in 20°C [52].

Chemical compound	Solubility (gr/lit)
K_2SO_4	111
Na_2SO_4	440
$NaNO_3$	740
KNO_3	316

According to Table 9, although the solubility of K2SO4 as a product of KOH in sulphuric acid (Eq. 1) is less than Na_2SO_4 as a product of NaOH in sulphuric acid (Eq.2), the residual mass of KOH mixtures in sulphuric acid was less than NaOH mortars. It can be inferred that permeability had a higher effect on sulphuric acid-exposed specimens than solubility. In contrast, in the nitric acid environment, the solubility of NaNO3 as a product of NaOH and nitric acid (Eq.3) was higher than KNO3 as a product of KOH and nitric acid (Eq.4) and subsequently, NaOH mixtures in nitric acid had a lower residual mass compared to KOH. Therefore, it can be concluded that in mixtures exposed to sulphuric acid, permeability had a significant role in the durability of mixtures while solubility was the dominant effect with respect to mixtures exposed to the nitric acid.

$$H_2SO_4 + KOH \rightarrow K_2SO_4 + H_2O \quad (1)$$

$$H_2SO_4 + NaOH \rightarrow Na_2SO_4 + H_2O \quad (2)$$

$$HNO_3 + NaOH \rightarrow NaNO_3 + H_2O \quad (3)$$

$$HNO_3 + KOH \rightarrow H_2O + KNO_3 \quad (4)$$

4. Conclusions

This study investigated the effect of using VPP as a replacement of GGBFS in AASP mortars. For this purpose, 10% VPP was substituted for GGBFS (by mass) and two types of alkaline activator (KOH and NaOH) were used to activate raw materials. The experimental investigations consisted of flowability, capillary water absorption, and MIP tests as well as durability against sulphuric acid and nitric acid by assessing visual inspection and changes of mass and compressive strength after exposure to the acidic environments. Besides, an XRD test was conducted to investigate the effects of acid environments on the mineral phases of the mortars. The results of four AASP mortars were compared to the cement-based mixture. According to the experimental results, the following general conclusions can be drawn from this study:

1) Inclusion of NaOH instead of KOH and replacing GGBFS with VPP reduced the flowability of AASP mortars. Thus, the mixture containing 6 molar NaOH and 10% VPP (Na6-Pu10) illustrated the lowest flowability contrary to K6-Pu0, among the studied AASP mortars.
2) Substitution of 10% VPP in AASP mortars reduced the capillary water absorption, especially at early ages (about 12%). Also, the capillary water absorption of AASP mortars was about 15% of OPC mortar.
3) Based on MIP results at 91 days, the micro-pores volume (100 nm to 50 μm) in the AASP mortars without VPP were less than those containing 10% VPP due to the less compactness of N-A-S-H type gel compared to C-A-S-H gel. In addition, AASP mortars containing NaOH showed a denser microstructure than those containing KOH.
4) According to the visual inspection results, AASP mortar specimens in sulphuric acid remained structurally intact, and the formation of a hard surface layer reduced the permeation of acid to the inner parts; however, in nitric acid, relatively high porosity and crystallization were observed near the surface of specimens.
5) There was no significant difference between mixtures with and without VPP in terms of mass and compressive strength changes in exposure to acidic environments, except for the mixture containing KOH in sulphuric acid. This difference was attributed to its higher permeability.
6) Although AASP activated by NaOH had better resistance in sulphuric acid in terms of mass change, in nitric acid solution, KOH-activated specimens revealed better performance in terms of mass and compressive strength change.
7) In mixtures exposed to sulphuric acid, permeability had a significant role in the durability of mixtures, while the solubility of reaction products had a prominent effect in mixtures exposed to nitric acid.
8) XRD analysis indicated that sulphuric acid had a higher effect on AASP mortars than those exposed to nitric acid, due to more changes in the composition of the mortars. This change in composition was associated with the expansion and subsequent destruction of mortar samples.

Overall, it can be concluded that employing 10% VPP had no significant effect on the durability of AASP mortars

against mineral acid attack; nevertheless, it is recommended to be used as a raw material with the aims of sustainability. It is also recommended to use NaOH to activate samples exposed to sulphuric acid and KOH for activation of nitric acid-exposed specimens.

Acknowledgements

This research was supported by the Iran National Science Foundation (INSF). The authors gratefully acknowledge financial support from the INSF. The authors also would like to appreciate the supervision and help of the late Professor Ali Akbar Ramezanianpour (1951-2021) in this study.

References

1. Senhadji, Y., et al., *Influence of natural pozzolan, silica fume and limestone fine on strength, acid resistance and microstructure of mortar.* Powder technology, 2014. **254**: p. 314-323.
2. Chen, K., et al., *Geopolymer concrete durability subjected to aggressive environments–a review of influence factors and comparison with ordinary Portland cement.* Construction and Building Materials, 2021. **279**: p. 122496.
3. Najimi, M., N. Ghafoori, and M. Sharbaf, *Alkali-activated natural pozzolan/slag mortars: A parametric study.* Construction and Building Materials, 2018. **164**: p. 625-643.
4. Provis, J.L. and J.S.J. Van Deventer, *Geopolymers: structures, processing, properties and industrial applications*. 2009: Elsevier.
5. Pacheco-Torgal, F., et al., *Durability of alkali-activated binders: a clear advantage over Portland cement or an unproven issue?* Construction and Building Materials, 2012. **30**: p. 400-405.
6. Fernando, P.-T., C.-G. João, and J. Said, *Durability and environmental performance of alkali-activated tungsten mine waste mud mortars.* Journal of Materials in Civil Engineering, 2010. **22**(9): p. 897-904.
7. Ariffin, M., et al., *Sulfuric acid resistance of blended ash geopolymer concrete.* Construction and building materials, 2013. **43**: p. 80-86.
8. Bakharev, T., *Resistance of geopolymer materials to acid attack.* Cement and concrete research, 2005. **35**(4): p. 658-670.
9. Allahverdi, A. and F. Škvára, *Nitric acid attack on hardened paste of geopolymeric cements, part I.* Ceramics-Silikáty, 2001. **45**(3): p. 81-88.
10. Allahverdi, A. and F. Skvara, *Sulfuric acid attack on hardened paste of geopolymer cements-Part 1. Mechanism of corrosion at relatively high concentrations.* Ceramics Silikaty, 2005. **49**(4): p. 225.
11. Thokchom, S., P. Ghosh, and S. Ghosh, *Acid resistance of fly ash based geopolymer mortars.* International Journal of Recent Trends in Engineering, 2009. **1**(6): p. 36.
12. Thokchom, S., P. Ghosh, and S. Ghosh, *Durability of fly ash geopolymer mortars in nitric acid–effect of alkali (Na2O) content.* Journal of Civil Engineering and Management, 2011. **17**(3): p. 393-399.
13. Bernal, S.A., et al., *Performance of alkali-activated slag mortars exposed to acids.* Journal of Sustainable Cement-Based Materials, 2012. **1**(3): p. 138-151.
14. Palankar, N., A.R. Shankar, and B. Mithun, *Durability studies on eco-friendly concrete mixes incorporating steel slag as coarse aggregates.* Journal of cleaner production, 2016. **129**: p. 437-448.
15. Blaakmeer, J. *Diabind: An alkali-activated slag fly ash binder for acid-resistant concrete*. in *Fuel and Energy Abstracts*. 1995.
16. Allahverdi, A., E.N. Kani, and M. Yazdanipour, *Effects of blast-furnace slag on natural pozzolan-based geopolymer cement.* Ceramics-Silikáty, 2011. **55**(1): p. 68-78.
17. Robayo, R., R.M. De Gutiérrez, and M. Gordillo, *Natural pozzolan-and granulated blast furnace slag-based binary geopolymers.* Materiales de Construcción, 2016. **66**(321): p. e077-e077.
18. Nadoushan, M.J. and A.A. Ramezanianpour, *The effect of type and concentration of activators on flowability and compressive strength of natural pozzolan and slag-based geopolymers.* Construction and Building Materials, 2016. **111**: p. 337-347.
19. Allahverdi, A., K. Mehrpour, and E.N. Kani, *Investigating the possibility of utilizing pumice-type natural pozzonal in production of geopolymer cement.* Ceramics silikaty, 2008. **52**(1): p. 16.
20. *ASTM C778-17, Standard Specification for Standard Sand, ASTM International, West Conshohocken, PA, 2017,.*
21. *ASTM C150 / C150M-20, Standard Specification for Portland Cement, ASTM International, West Conshohocken, PA, 2020.*
22. Nadoushan, M.J., A.A. Ramezanianpour, and S.M. Kheirandish. *Mechanical and Durability Properties of Alkali Activated Slag for Sustainable Concrete*. in *Fourth International Conference on Sustainable Construction Materials and Technologies (SCMT4), The University of Navada, Las Vegas, USA*. 2016.

23. *ASTM C305-20, Standard Practice for Mechanical Mixing of Hydraulic Cement Pastes and Mortars of Plastic Consistency, ASTM International, West Conshohocken, PA, 2020.*
24. *ASTM C1437-20, Standard Test Method for Flow of Hydraulic Cement Mortar, ASTM International, West Conshohocken, PA, 2020.*
25. *BS EN 480-5, "Admixtures for concrete, mortar and grout test methods- Part 5: Determination of capillary absorption", British Standard, 2005.*
26. *ASTM C109 / C109M-20b, Standard Test Method for Compressive Strength of Hydraulic Cement Mortars (Using 2-in. or [50 mm] Cube Specimens), ASTM International, West Conshohocken, PA, 2020.*
27. Ramezanianpour, A.A. and M.A. Moeini, *Mechanical and durability properties of alkali activated slag coating mortars containing nanosilica and silica fume.* Construction and Building Materials, 2018. **163**: p. 611-621.
28. Hanjitsuwan, S., et al., *Effects of NaOH concentrations on physical and electrical properties of high calcium fly ash geopolymer paste.* Cement and Concrete Composites, 2014. **45**: p. 9-14.
29. Abubakr, A., A. Soliman, and S. Diab, *Effect of activator nature on the impact behaviour of Alkali-Activated slag mortar.* Construction and Building Materials, 2020. **257**: p. 119531.
30. Yang, K.-H., et al., *Properties of cementless mortars activated by sodium silicate.* Construction and Building Materials, 2008. **22**(9): p. 1981-1989.
31. Rodríguez, E., et al., *Alternative concrete based on alkali-activated slag.* Materiales de Construcción, 2008. **58**(291): p. 53-67.
32. Bernal, S.A., et al., *Effect of binder content on the performance of alkali-activated slag concretes.* Cement and concrete research, 2011. **41**(1): p. 1-8.
33. Bernal, S., et al., *Performance of an alkali-activated slag concrete reinforced with steel fibers.* Construction and building Materials, 2010. **24**(2): p. 208-214.
34. Adam, A., et al., *Strength, sorptivity and carbonation of geopolymer concrete.* Challenges, Opportunities and Solutions in Structural Engineering and Construction, 2010: p. 563-568.
35. Valente, M., M. Sambucci, and A. Sibai, *Geopolymers vs. cement matrix materials: how nanofiller can help a sustainability approach for smart construction applications—a review.* Nanomaterials, 2021. **11**(8): p. 2007.
36. Davidovits, J., *Geopolymer, green chemistry and sustainable development solutions: proceedings of the world congress geopolymer 2005*. 2005: Geopolymer Institute.
37. Chi, M. and R. Huang, *Binding mechanism and properties of alkali-activated fly ash/slag mortars.* Construction and building materials, 2013. **40**: p. 291-298.
38. Ismail, I., et al., *Influence of fly ash on the water and chloride permeability of alkali-activated slag mortars and concretes.* Construction and Building Materials, 2013. **48**: p. 1187-1201.
39. Salehi, H. and M. Mazloom, *Opposite effects of ground granulated blast-furnace slag and silica fume on the fracture behavior of self-compacting lightweight concrete.* Construction and Building Materials, 2019. **222**: p. 622-632.
40. Kong, D., et al., *Effect and mechanism of colloidal silica sol on properties and microstructure of the hardened cement-based materials as compared to nano-silica powder with agglomerates in micron-scale.* Cement and Concrete Composites, 2019. **98**: p. 137-149.
41. Cook, R.A. and K.C. Hover, *Mercury porosimetry of hardened cement pastes.* Cement and Concrete research, 1999. **29**(6): p. 933-943.
42. Cui, L. and J.H. Cahyadi, *Permeability and pore structure of OPC paste.* Cement and Concrete Research, 2001. **31**(2): p. 277-282.
43. Fang, G. and M. Zhang, *Multiscale micromechanical analysis of alkali-activated fly ash-slag paste.* Cement and Concrete Research, 2020. **135**: p. 106141.
44. Fernández-Jiménez, A., A. Palomo, and M. Criado, *Alkali activated fly ash binders. A comparative study between sodium and potassium activators.* Materiales de Construcción, 2006. **56**(281): p. 51-65.
45. Shi, C., *Corrosion resistance of alkali-activated slag cement.* Advances in cement research, 2003. **15**(2): p. 77-81.
46. Allahverdi, A. and F. SKVARA, *Acidic corrosion of hydrated cement based materials. Part 1.: Mechanism of the phenomenon.* Ceramics (Praha), 2000. **44**(3): p. 114-120.
47. Bakharev, T., J.G. Sanjayan, and Y.-B. Cheng, *Resistance of alkali-activated slag concrete to acid attack.* Cement and Concrete research, 2003. **33**(10): p. 1607-1611.
48. Türker, H.T., et al., *Microstructural alteration of alkali activated slag mortars depend on exposed high temperature level.* Construction and Building Materials, 2016. **104**: p. 169-180.
49. Elyamany, H.E., A.E.M.A. Elmoaty, and A.R.A. Diab, *Sulphuric Acid Resistance of Slag Geopolymer Concrete Modified with Fly Ash and Silica Fume.* Iranian Journal of Science and Technology, Transactions of Civil Engineering, 2021. **45**(4): p. 2297-2315.
50. Singh, A., et al., *Effect of nitric acid on Rice Husk Ash steel fiber reinforced concrete.* Materials Today: Proceedings, 2020. **27**: p. 995-1000.

51. Moodi, F., S. Norouzi, and P. Dashti, *Mechanical properties and durability of alkali-activated slag repair mortars containing silica fume against freeze-thaw cycles and salt scaling attack.* Advances in concrete construction, 2021. **11**(6): p. 493-505.
52. Patnaik, P., *Handbook of inorganic chemicals*. Vol. 529. 2003: McGraw-Hill New York.